Modeling of packed bed column studies for the removal of Cu(II) using polypyrrole alumina iron oxide nanocomposite

P.N. Mary Lissy[a],*, G. Madhu[b], Roy M. Thomas[c]

[a]*Department of Civil Engineering, Muthoot Institute of Technology and Science, Varikoli 9895210149, India,*
email: marylissypn@gmail.com
[b]*Department of Chemical Engineering, Cochin University of Science & Technology, Kalamasserry, Ernakulam 9447366900,*
India, email: profmadhugopal@gmail.com
[c]*Department of Civil Engineering, Cochin University of Science & Technology, Kalamasserry 9447147194, Ernakulam,*
India, email: roymthomas2007@gmail.com

ABSTRACT

The performance of fixed-bed column with polypyrrole alumina iron oxide nanocomposite was studied under various conditions to investigate the effects of parameters such as bed height, flow rate and initial concentration in the removal of Cu^{2+} ions from aqueous media. The experimental studies reveal that the breakthrough time was increasing with an increase in bed height. Maximum removal with higher bed height is achieved due to the increase in the adsorption sites providing a larger surface area thereby leading to an increase in the volume of the treated solution. A higher flow rate produced a steeper curve with early breakthrough time and resulted in less adsorption intake. The adsorbent capacity was exhausted faster due to the saturation of binding sites in the case of higher flow rate and inlet concentration. Extended breakthrough time was obtained when inlet concentration was decreased, indicating that more amount of the solution could be treated. A decrease in the mass transfer coefficient was observed at lower concentration causing slower transport. Mathematical modeling of the adsorption column was studied with various models like Thomas model, Yoon–Nelson model and Adams–Bohart model to identify the best model and found Yoon–Nelson model fits well with the experimental data.

Keywords: Adams–Bohart model; Thomas model; Yoon–Nelson model; Polypyrrole; Nanoadsorbent

1. Introduction

Metal pollutants are increasing in the water resources at an alarming rate causing a threat to living beings. The addition of toxic heavy metals like chromium, copper, zinc, lead and cadmium is adversely affecting the environment. Rapid industrialization is the main cause of the occurrence of Cu(II). Increased levels of toxic metals can cause severe damage to the circulatory and nervous systems of human beings [1]. Removal of toxic Cu(II) ions from wastewater are essential for health and environmental protection.

As per IS 10500:2012, the acceptable limit of copper in drinking water is 0.05 mg/L. Several physicochemical processes such as membrane technology, flocculation, coagulation, electrodialysis, reverse osmosis, etc are available for the treatment [2]. But these techniques have certain limitations such as less economic feasibility, less percentage removal and the difficulty to dispose. Among the present conventional techniques, the adsorption process is the most suitable method because of its high efficiency and economic consideration. Many adsorbents like activated carbon, silicates, natural zeolite, chitosan polymer and biomass have

* Corresponding author.

been used for the removal of heavy metal ions with certain limitations [3]. Hence the need for a better adsorbent possessing high removal efficiency and adsorption capacity has led to this research work. Polypyrrole coated nanocomposite with high conductivity, easy preparation and environmental stability is found to be one of the most promising conducting polymers in the removal of toxic metal ions [4,5].

A fixed-bed column is an industrially viable method for the removal of various contaminants from wastewater and its performance is studied by the breakthrough curve representing the influent–effluent concentration vs. time [6]. The adsorption mechanism consists of axial dispersion, film diffusion resistance, sorption equilibrium with sorbent and intraparticle diffusion resistance which includes both surface and pore diffusion [7]. Using nanocomposite as adsorbent, copper solutions of corresponding concentrations are allowed to continuously flow through the bed of the adsorbent at a constant rate [8]. As the adsorbate is continuously in contact with a given quantity of adsorbent in a fixed-bed column system this method proves to be more feasible considering industrial parameters.

2. Materials and methods

2.1. Adsorbent

The alumina iron oxide nanocomposite (Al_2O_3–Fe_2O_3) was prepared by blending the required amount of 3.9 g $FeSO_4$ and 7.8 g $FeCl_3$ in 200 mL distilled water into which activated alumina of 35.1 g was added with constant heating at 70°C. The weight ratio of activated alumina to iron oxide was chosen as 3:1 to prevent a decrease in the adsorption capacity of synthesized nanocomposites due to the increased content of iron oxide. A solution of 10% NaOH was added drop-wise to precipitate the iron oxides and the obtained precipitate was cooled, filtered and dried at room temperature of 32°C to get the product [9]. Chemical polymerization of pyrrole using ferric chloride as chemical oxidant and water as solvent was carried out with 5 g ferric chloride in 100 mL distilled water and a uniform solution was made using a magnetic mixer. Alumina iron oxide nanocomposite of 1 g along with 1 mL pyrrole monomer was added into the solution and the response was observed for 4 h at an ambient temperature of 32°C. Thereafter the filtered product was kept in an oven at a temperature of 60°C for 24 h to obtain polypyrrole alumina iron oxide nanocomposite (PPy/Al_2O_3-Fe_2O_3) [10].

2.2. Adsorbate

A copper stock solution of 1,000 mg/L was prepared by adding the required copper sulfate in distilled water. Dilution was done to prepare samples of varying concentrations of 200 to 1,000 mg/L and the pH value was adjusted by adding 0.1 N HCl and 0.1 N NaOH. Experimental studies reveal that as pH increases conductivity increases steadily. Around pH 8, conductivity remains almost constant and not very appreciable. Cu^{++} on hydrolysis produces ions such as $Cu(OH)^+$, $Cu(OH)_2$, $Cu(OH)_3^-$, $Cu(OH)_4^{2-}$. In acidic pH, species $Cu(OH)^+$, $Cu(OH)_2$ only exist. Since the solution contains the fastest-moving H^+ ions, conductivity would be higher. As the pH value increases above 4, bulkier ions $Cu(OH)_3^-$ and $Cu(OH)_4^{2-}$ could exist with lesser density. Similar results were obtained at higher alkaline pH and hence it can be concluded that around pH 8, hydrolysis of Cu^{++} has no much effect. Copper concentrations in the solution before and after adsorption were determined from a standard calibration curve generated using a direct UV visible spectrophotometric method with a wavelength corresponding to maximum absorbance (λ_{max}) of 645 nm [11].

2.3. Fixed-bed column studies

Packed bed column study analysis was done in a glass column of 2.5 cm diameter and a height of 1 foot. Synthesized polypyrrole alumina iron oxide nanocomposite was placed at the center of the column supported with glass wool. The up-flow continuous fixed-bed adsorption technique was used to study the removal process. All the experiments were carried out with Cu^{2+} solutions having a pH value of 8 which was found as optimum through batch mode adsorption studies. Effects of various parameters like flow rates of 10, 15, 20 and 25 mL/min, bed depth of 1, 2, 3 and 4 cm and metal concentration of 200, 400, and 600 mg/L were investigated. Samples were tested every 5 min to know the metal uptake by the nanocomposite. The pseudo-second-order reaction rate model described the adsorption data adequately with the good and statistically significant coefficient of determination. The sorption capacity of nanocomposite increased with increasing adsorbate concentration in the pseudo-second-order model. Thermodynamic parameters obtained from the batch mode adsorption studies using PPy/Al_2O_3-Fe_2O_3 nanocomposite confirm that the maximum removal has occurred through physical adsorption process and the negative values of Gibbs free energy change ($\Delta G°$), low value of enthalpy change ($\Delta H°$) and energy of activation (E_a) indicates the feasibility of the process.

2.4. Mathematical modeling

The performance of a fixed-bed column is analyzed through the concept of a breakthrough curve [8]. The operation and dynamic response of an adsorption column are determined through the time for breakthrough curve appearance and its shape. The loading behavior of copper concentration to be adsorbed from solution in a fixed bed column is usually expressed as C_t/C_0 as a function of time or quantity of the effluent for a fixed-bed height. The value of q_{total} for a given feed concentration and flow rate corresponds to the area under the curve generated with adsorbed concentration C_{ad} ($C_{ad} = C_0 - C_t$) (mg/L) vs. t (min) and can be calculated from the following equation.

$$q_{total} = \frac{Q}{1,000} \int_{t=0}^{t=t_{total}} C_{ad} dt \tag{1}$$

where q_{total} is the maximum bed capacity in mg, the inlet flow rate in mL/min and the adsorbed concentration in ppm is denoted as Q and C_{ad} respectively. The value of the integral is calculated from the area under the plot of adsorbed concentration vs. time.

M_{total} in mg is the total quantity of metal ions passed through the column, C_0 is initial dye concentration in ppm, the volumetric flow rate is denoted as Q (mL/min) and the total flow time is represented as t_{total} (min). M_{total} is calculated using the following equation.

$$M_{total} = \frac{C_0 Q t_{total}}{1,000} \tag{2}$$

Total percentage of metal ion removal is given by the following equation:

$$\%Removal = \left(\frac{q_{total}}{M_{total}}\right) \times 100 \tag{3}$$

where q_{total} is the maximum bed capacity in mg, M_{total} is the total amount of metal ions sent to the column in mg.

Equilibrium metal ion uptake in the column is given by the following equation:

$$q_{eq} = \frac{q_{total}}{X} \tag{4}$$

where q_{eq} is the equilibrium metal ion uptake in mg/g and X is the amount of nanocomposites in the column in g.

Adsorbed concentration of metal ions at equilibrium is found by the following equation:

$$C_{eq} = \left(M_{total} - q_{total}\right) \times \frac{1,000}{V_{eff}} \tag{5}$$

where C_{eq} is the equilibrium adsorbed concentration in ppm.

The prediction of the concentration-time profile or breakthrough curve is required for the successful design of a packed bed column adsorption system. Kinetic models were used to express the dynamic process of the column mode [12].

2.4.1. Thomas model

The most common method used in the column performance theory is the Thomas model [13]. The experimental values obtained from continuous mode column studies were used to calculate the maximum solid-phase concentration of copper and chromium on the adsorbent. The kinetic model developed by Thomas is used to find the adsorption rate constant is shown in Eq. (6).

$$\frac{C_f}{C_0} = \frac{1}{1 + \exp\left(\left(\frac{K_{th}}{F}\right)\left(q_0 x - C_0 V_{eff}\right)\right)} \tag{6}$$

where C_f and C_0 in mg/L are the effluent and influent concentrations, Thomas rate constant in mL/mg min is denoted as K_{th}, maximum adsorption in mg/g is shown as q_0, x is the quantity of adsorbent in the column (g), feed flow rate is shown as F in mL/min and the effective volume of the solution is expressed as V_{eff} in mL/min.

2.4.2. Adams–Bohart model

The relationship between C_f/C_0 and time is explained using a fundamental equation established by Adams–Bohart model [14]. This model assumes that the rate of adsorption is proportional to the adsorbent capacity and the adsorbing species concentration. The breakthrough curve in the initial part is explained using this model and is expressed in Eq. (7).

$$\ln\left(\frac{C_f}{C_0}\right) = K_{ab}C_0 t - \frac{K_{ab}N_0 Z}{U_0} \tag{7}$$

where C_f and C_0 in mg/L are the effluent and initial concentrations respectively, kinetic constant in L/mg min is denoted as K_{ab}, the capacity of adsorption is N_0 in g/L, bed depth in the column is represented as Z (m), t is time in minutes and U_0 is the speed of gas out in m/s.

The properties of operational parameters of the fixed bed column can be evaluated from a plot of C_f/C_0 against time at a given bed height and flow rate using the non-linear regressive method.

2.4.3. Yoon–Nelson model

This model is based on the assumption that the decreased rate in the probability of adsorption for each adsorbate molecule is proportional to the probability of adsorbate adsorption and adsorbate breakthrough on the adsorbent [15]. The Yoon–Nelson model is applied to check the experimental data which is expressed in Eq. (8).

$$\frac{C_f}{C_0 - C_f} = \exp\left(K_{YN}t - \tau K_{YN}\right) \tag{8}$$

The time needed for 50% adsorbate breakthrough is denoted as τ in min, the sampling time is shown as t (min), and K_{YN} is the rate constant (min^{-1}).

3. Results and discussion

3.1. Characterization of nanoadsorbents

Characterization of nanoparticle using scanning electron microscopy (SEM), transmission electron microscopy (TEM), Brunauer–Emmett–Teller (BET), X-ray diffraction analysis (XRD) and Fourier-transform infrared spectroscopy (FTIR) is done to collect information about chemical composition and physical properties such as size, shape, surface properties, crystallinity and dispersion state [16].

3.1.1. SEM and TEM analysis

SEM analysis is conducted to determine the surface morphology of the particles. Figs. 1 and 2 represent the SEM image of the synthesized nanocomposite before and after adsorption of copper ions showing a difference in the surface morphology of the two images confirming that the adsorption has taken place. TEM was used to find the nature of magnetic nanoparticles in the nanocomposite produced. The produced composite showed uniform
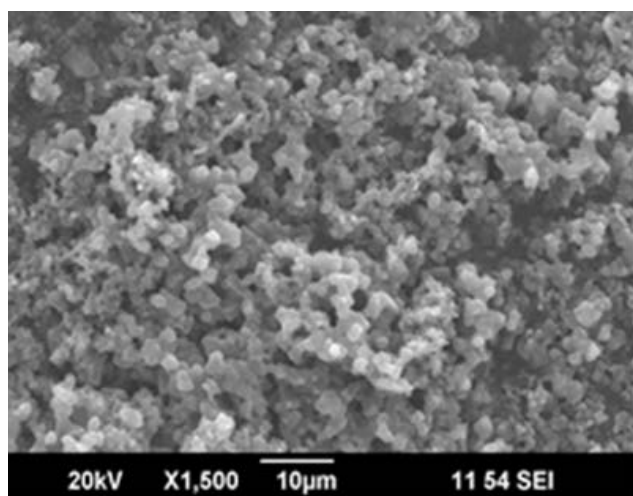
Fig. 1. SEM analysis before adsorption.
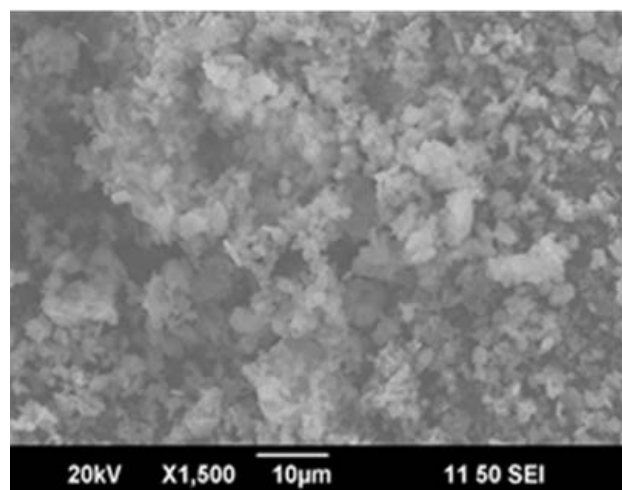
Fig. 2. SEM analysis after adsorption.

spherical nanoparticles in the form of nanoclusters as shown in Fig. 3.

3.1.2. BET analysis

BET analysis of polypyrrole alumina iron oxide nanocomposite using nitrogen isotherm was done to determine the surface area and the pore structure as a function of relative pressure. The specific surface area and average pore size of PPy/Al_2O_3-Fe_2O_3 nanocomposite determined using BET analysis is 13.6402 m^2/g and 40.31 nm respectively. The micropore area and micropore volume were calculated as 27.8722 m^2/g and 0.01435 cm^3/g respectively. Fig. 4 represents the adsorption plot indicating that the nanocomposite belongs to type IV isotherm which confirms that most of the particles are mesoporous materials with a size less than 50 nm.

3.1.3. XRD analysis

XRD analysis was performed for phase identification of a crystalline structure. The crystallite sizes were found to be
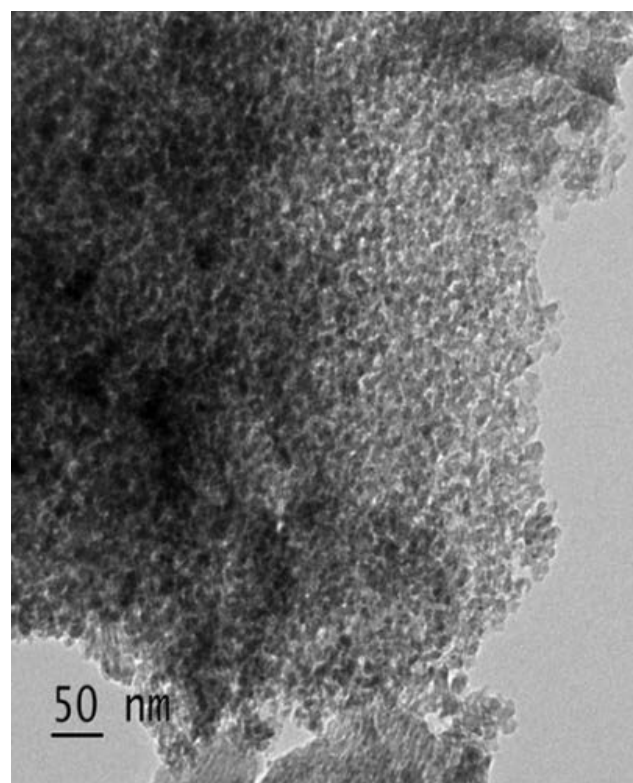
Fig. 3. TEM analysis.

23.66, 24.89, 23.75, 24.61, 13.26, 22.35 and 21.66 nm for the respective peaks using the Scherrer equation. The average particle size as per XRD analysis was found to be 20.03 nm. In Fig. 5, the XRD pattern represents the crystal structure of the PPy/Al_2O_3-Fe_2O_3 nanocomposite.

The broad peak resembles the scattering of X-ray from the PPy chain. The broad peak at 2θ value of 24.285 indicates the presence of polypyrrole having amorphous behavior of the polymer [17] and the values of 33.287, 35.801 and 54.135 corresponds to the presence of –Fe_2O_3 phase with rhombohedral structure (JCPDS 79-1741). The peaks at 40.98 and 64.097 show the presence of the AlO(OH) phase with orthorhombic structure [18]. All other diffraction peaks indicate the presence of α-Al_2O_3 (JCPDS FILE NO-(42-1468) and α-Fe_2O_3 (JCPDS FILE NO (79-1741).

3.1.4. FTIR analysis

The characterization of nanocomposite was done using FTIR analysis to identify the chemical bonds present in the nanocomposite. The spectrum of PPy/Al_2O_3-Fe_2O_3 nanocomposite before copper ion adsorption as shown in Fig. 6 indicates that the band at 1,567.93 cm^{-1} is due to C–C and C=C backbone stretching of the nanocomposite.

The band at 1,398.96 cm^{-1} corresponds to C–N stretching. The band at 1,004.41 cm^{-1} corresponds to C–H stretching and N–H wagging. The band at 798.41 cm^{-1} is attributed to C–H wagging vibration. Thus it reflects that all the corresponding bands of PPy/Al_2O_3-Fe_2O_3 nanocomposite are present in the spectrum. The bands corresponding to Fe–O, Al–O and Fe–Al vibrations are also present.
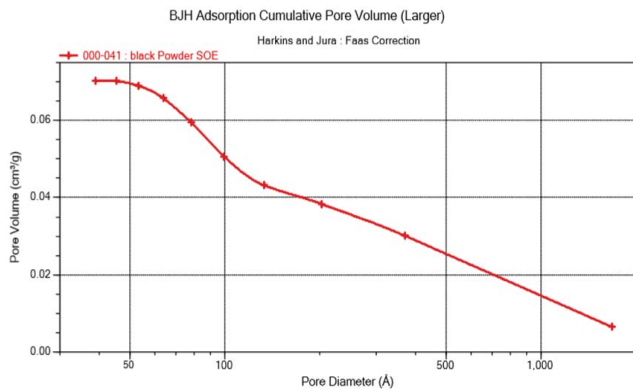
Fig. 4. BET analysis.

From FTIR analysis of nanocomposite after adsorption, as shown in Fig. 7, it is clearly visible that shift has taken place after the adsorption of copper using the prepared nanocomposite. The bands at 1,567.93; 1,398.96; 1,004.41; 798.41; 686.61 and 480.16 cm^{-1} observed before the adsorption process have shifted to 1,542.19; 1,219.95; 895.21, 783.17, 677.87 and 405.14 cm^{-1} respectively after adsorption of copper ions. The band at 1,542.19 and 1,219.95 cm^{-1} corresponds to C–N amide II band and CH$_2$ twisting respectively. The band at 895.21 cm^{-1} is attributed to CH$_2$ wagging vibrations. The bands at 783.17, 677.87 and 405.14 cm^{-1} correspond to C–H in out of plane deformation and C=C twisting. All these shifts confirm the adsorption of copper ions by PPy/Al$_2$O$_3$-Fe$_2$O$_3$ nanocomposite.

3.2. Effect of bed height

The breakthrough curve was obtained from the experimental studies for the adsorption of copper ions onto PPy/Al$_2$O$_3$-Fe$_2$O$_3$ nanocomposites for varying bed heights of 1, 2, 3 and 4 cm. The adsorbate feed flow rate of 15 mL/min and 400 mg/L inlet concentration were kept constant.

From Fig. 8, it is observed that the breakthrough time was increasing with an increase in the bed height. Maximum uptake was found when the bed height was 4 cm. It is due to the increase in the adsorption sites due to the increase in the quantity of the adsorbent. Hence the mass transfer zone was increased. In a column with fixed bed media, the direction of the mass transfer zone is from the entry-level of the bed towards the exit level [19]. Therefore in the case of the same influent concentration and packed media, bed height increase will cause the mass transfer zone to reach the exit after an extended breakthrough time. For a greater bed height, an increase of adsorbent provided a larger surface area thereby leading to an increase in the volume of the solution.

3.3. Flow rate effect

The effect of flow rate on the uptake of copper ions were studied by changeable flow rates of 10, 15, 20 and 25 mL/min at a constant bed height of 2 cm and inlet concentration of 400 mg/L. The curve obtained from the plot C_t/C_0 vs. time showed that bigger contact time was obtained for a lower flow rate of 10 mL/min creating a shallow adsorption zone. The higher flow rate of 25 mL/min produced a steeper curve with early breakthrough time and resulted in less adsorption intake. The bed media was saturated early at a higher flow rate. It is clearly observed that the best performance of the column is obtained at a lower flow rate and higher residence time. Plots of the breakthrough curve at various times are depicted in Fig. 9.

3.4. Effect of initial concentration

The breakthrough curve for the adsorption of copper onto prepared nanocomposite was studied. Fig. 10 shows the
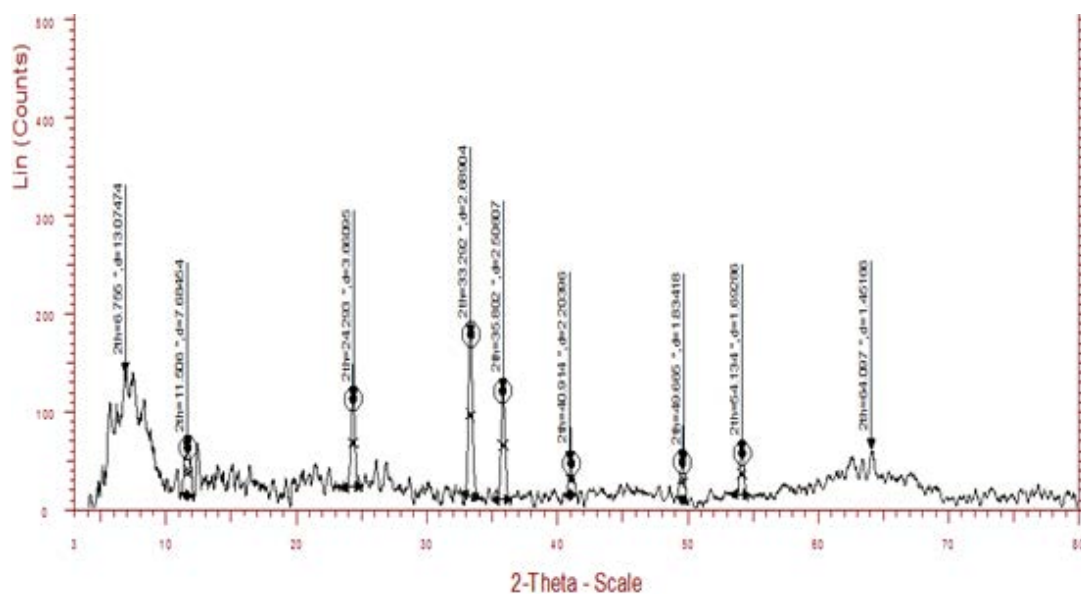
Fig. 5. XRD analysis of PPy/Al$_2$O$_3$-Fe$_2$O$_3$ nanocomposite.
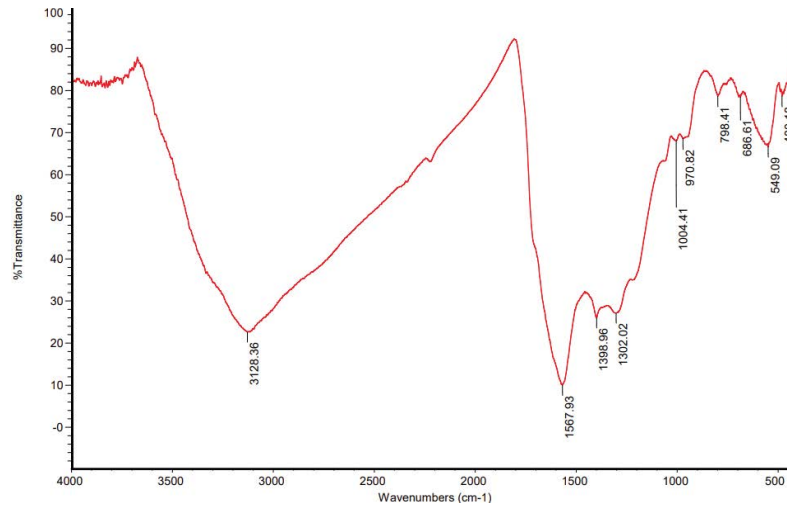
Fig. 6. FTIR analysis of PPy/Al$_2$O$_3$-Fe$_2$O$_3$ before adsorption.
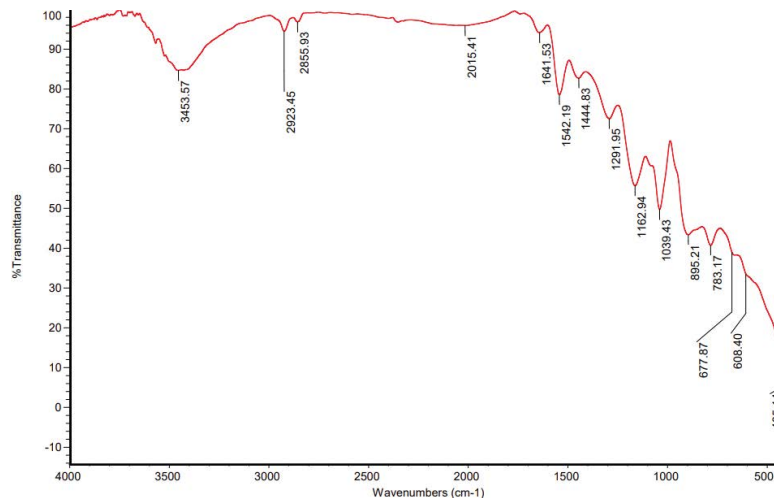
Fig. 7. FTIR analysis of PPy/Al$_2$O$_3$-Fe$_2$O$_3$ after adsorption.

effect of initial concentration on the breakthrough curves using a bed height of 2 cm and a flow rate of 15 mL/min.

An earlier breakthrough point was reached at a higher influent concentration of 600 mg/L when compared to the lowest concentration of 200 mg/L. The adsorbent capacity was exhausted faster due to the saturation of binding sites in the case of higher inlet concentration. An extended breakthrough curve was obtained when inlet concentration was decreased; indicating that more amount of the solution could be treated. A decrease in the mass transfer coefficient was observed at lower concentrations causing slower transport. The pH of the eluted solution was in the range of 7–8 for varying copper concentrations.

3.5. Mathematical models

3.5.1. Thomas model

Adsorption of copper ions onto a column packed by nanocomposite was studied using a mathematical model suggested by Thomas. Table 1 represents the model parameters calculated from the graphs obtained with $\ln((C_0/C_f)-1)$ vs. time. The adsorption data at various bed heights, flow rates and initial concentration was applied to estimate the kinetic coefficients for the adsorbent–adsorbate system. The coefficient of determination R^2 ranging from 0.946 to 0.996 indicates a linear relationship between the variables. The adsorption capacity q_0 decreased from 40.204 to 37.309 mg/g on increasing the influent concentration from 200 to 400 mg/L and showed the value increased from 37.309 to 48.85 mg/g when concentration increased from 400 to 600 mg/L. The adsorption capacity showed a decreasing trend while increasing the bed depths from 1 to 4 cm. Though the increase in bed depth may enhance the quantity of effluent treated, it reduces the amount of solute per unit adsorbent quantity. Studies using ethylamine modified chitosan carbonized rice husk composite beads also showed that the higher bed height contain more adsorbent with more binding sites making the breakthrough time
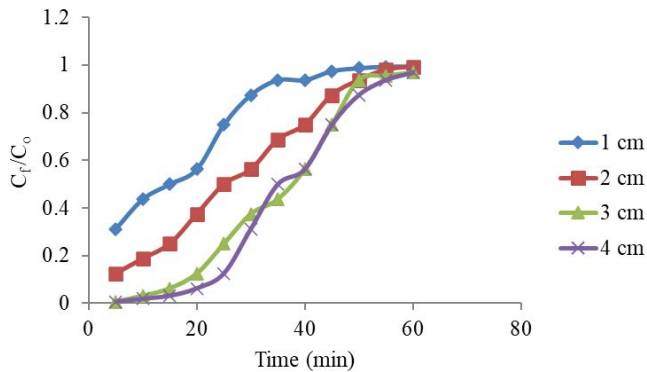
Fig. 8. Effect of bed height on breakthrough curves.
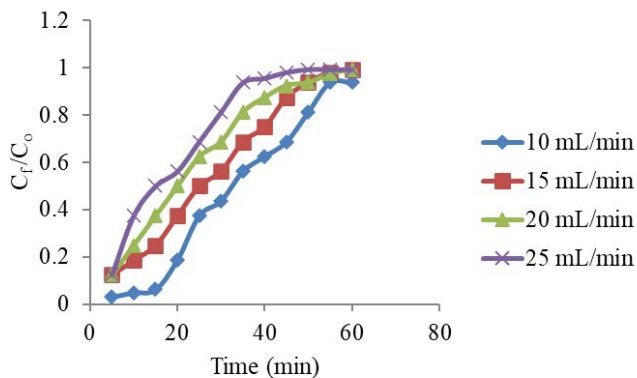
Fig. 9. Effect of flow rates on breakthrough curve.
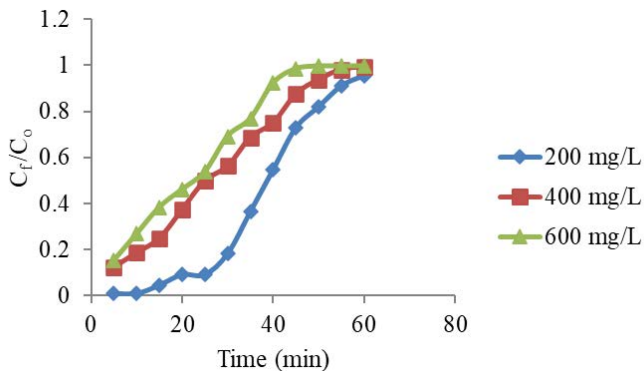
Fig. 10. Effect of initial concentration on breakthrough curve.

lesser [15]. The adsorption capacity was increasing from 34.805 to 42.102 mg/g as the flow rate increased from 10 to 25 mL/min.

Breakthrough curves with respect to the experimental data and theoretical data are shown in Fig. 11 for varying bed heights, flow rate and initial concentration.

3.5.2. Yoon–Nelson model

The constants of the Yoon–Nelson model, K_{YN} and τ were evaluated from the slope and intercept obtained from the graph $\ln(C_f/(C_0 - C_f))$ vs. time as shown in Fig. 12 and the

results are presented in Table 2. It was found from all the investigations that the adsorption capacity determined for both the theoretical and experimental studies showed similar results fitting well with Yoon–Nelson model.

On increasing the adsorbate concentration from 200 to 600 mg/L, the time required for 50% breakthrough τ decreased from 38.986 to 20.041 min. This may be due to the quick saturation of the adsorbent happened at a higher concentration. The results show that the increase in the flow rate from 10 to 25 mL/min decreased the value of τ from 34.805 to 16.841 min which corresponds to a decrease in the treated solution. An increase in the bed height increased the adsorption sites which in turn shows an increase in the τ value from 13.983 to 37.171 min. Thus the quantity of treated effluent increases.

Breakthrough curves predicted by Yoon–Nelson model for varying bed height, flow rate and initial concentration was compared with the experimental breakthrough curves as shown in Fig. 9.

3.5.3. Adams–Bohart model

Adams–Bohart model is applied directly to evaluate the adsorption system. The amount of copper ions adsorbed was found through the adsorption capacity coefficient N_0 (mg/L). With respect to the adsorbent amount and the quantity of treated copper solution, this factor was transformed to the adsorbent capacity packed in the column. Adams–Bohart model parameters obtained from the graph $\ln(C_f/C_0)$ vs. time are shown in Table 3.

The adsorption rate coefficient K_{ab} decreases from 45×10^{-5} to 5.17×10^{-5} L/mg min on increasing the influent concentration from 200 to 600 mg/L. The higher solute molecules form a greater concentration gradient when the concentration increases by which the adsorption rate coefficient decreases. Adsorption rate coefficient indicates the influent volume treated by unit volume of adsorbent at unit time. The adsorption rate coefficient decreases from 16×10^{-5} to 7×10^{-5} L/mg min when the flow rate increases from 10 to 25 mL/min. It was observed that when the bed height increased from 1 to 4 cm, K_{ab} coefficient increased from 4.8×10^{-5} to 23×10^{-5} L/mg min.

The experimental and calculated data are showing high variations as evident from regression coefficient values which concludes that this model is not fitting well to the experimental data. Breakthrough curves predicted by Adams–Bohart model for varying bed height, flow rate and initial concentration was compared with the experimental breakthrough curves as shown in Fig. 13.

The coefficient of determination obtained from the graph C_f/C_0 (experimental) vs. C_f/C_0 (theoretical) are presented in Table 4. The R^2 values obtained for Thomas model in case of varying bed heights and inlet concentrations are very less compared to the R^2 values obtained for varying flow rates. Hence Thomas model is not fitting well with the experimental data.

Similar trend was observed in the studies with brushite calcium phosphate in the removal of Cu(II) which shows that the linearization is not appropriate when using the pseudo-first-order, Adams–Bohart and Thomas models since it affects their error structure [20]. The coefficient
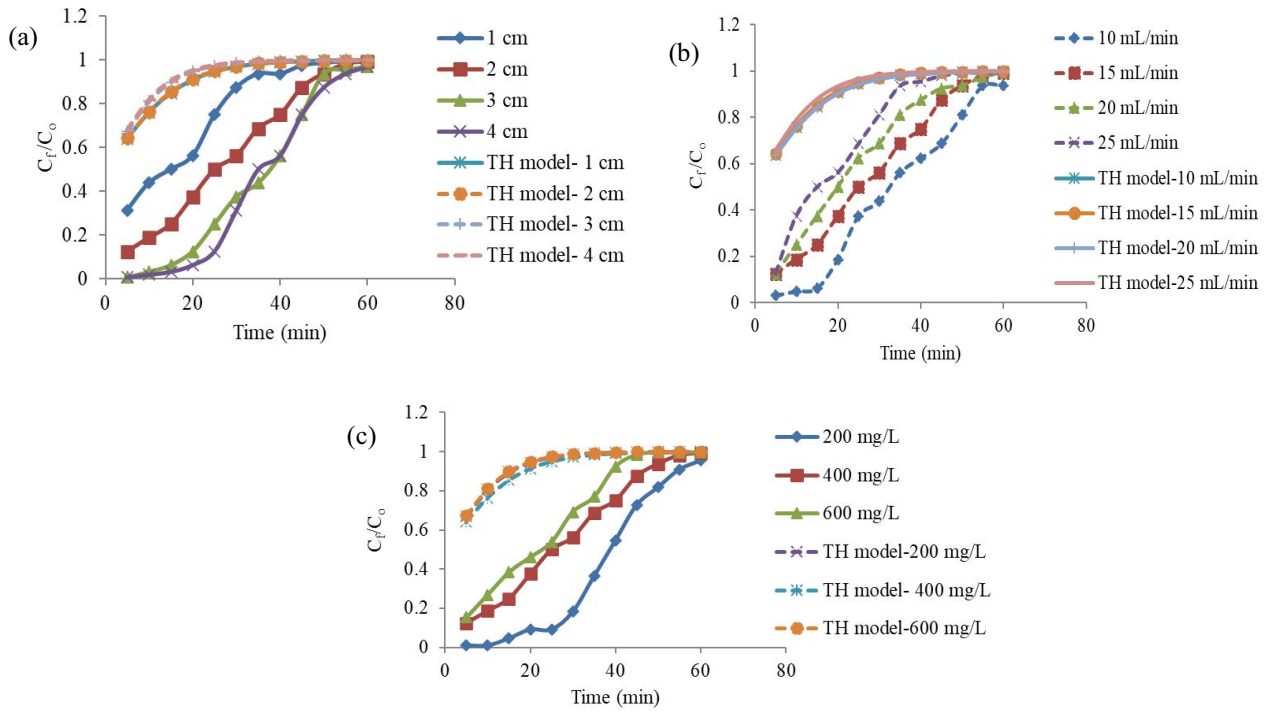
Fig. 11. (a–c) Experimental and theoretical breakthrough curves predicted by Thomas model.
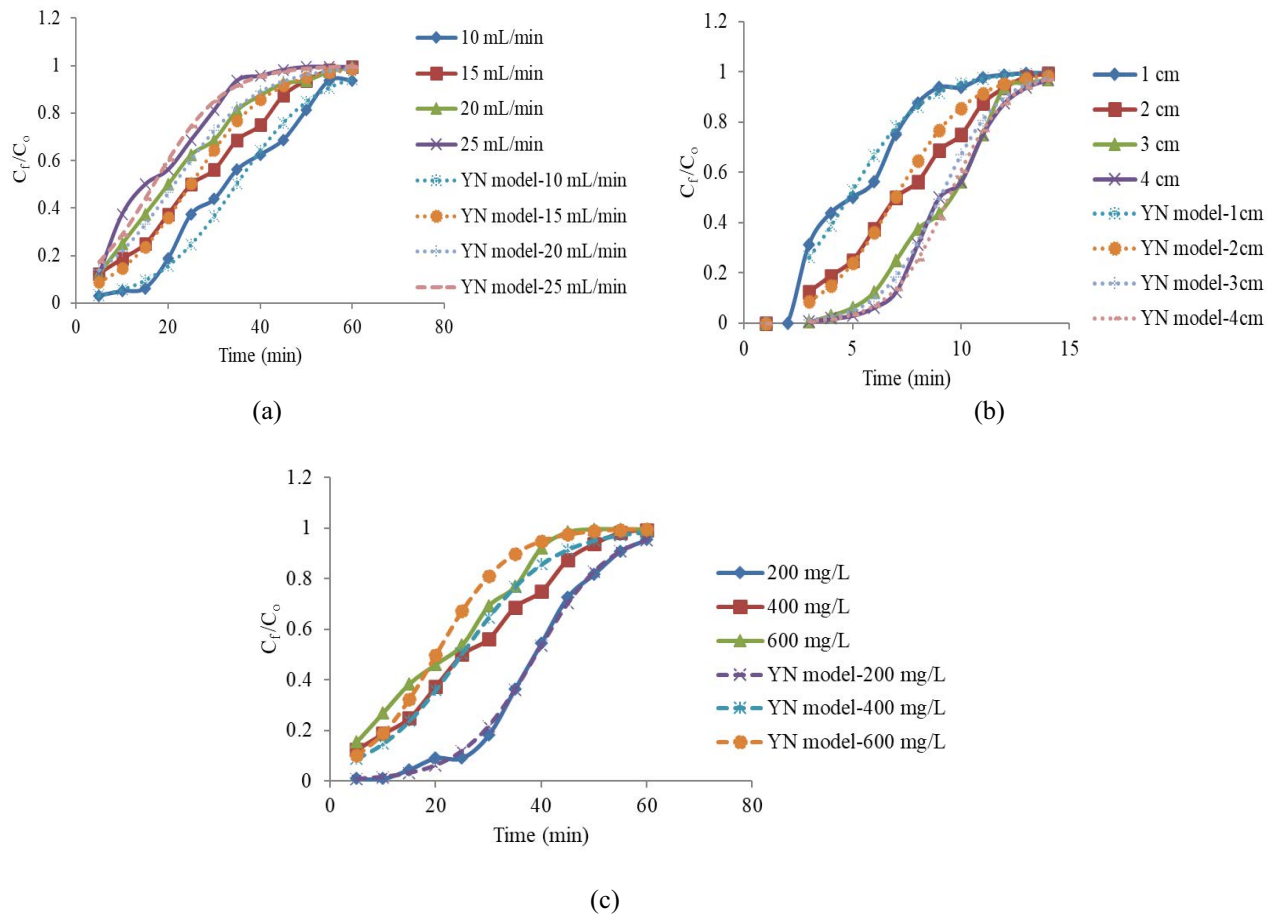
Fig. 12. (a–c) Experimental and theoretical breakthrough curves by Yoon–Nelson model.

Table 1
Thomas coefficient K_{th} and maximum solid-phase concentration q_0 for various bed height, flow rate and initial concentration

Influent concentration (mg/L)	Bed height (cm)	Flow rate (mL/min)	K_{th} (L/mg min) (10^{-5})	q_0 (mg/g)	R^2
400	1	15	28.75	41.947	0.984
400	2	15	29.50	37.309	0.956
400	3	15	36.50	35.164	0.98
400	4	15	38.00	27.878	0.996
400	2	10	28.25	34.805	0.975
400	2	15	29.50	37.309	0.956
400	2	20	28.00	42.482	0.978
400	2	25	33.00	42.102	0.975
200	2	15	52.00	40.204	0.989
400	2	15	29.50	37.309	0.956
600	2	15	22.46	48.850	0.946

Table 2
Parameters predicted by Yoon–Nelson model

Influent concentration (mg/L)	Bed height (cm)	Flow rate (mL/min)	K_{YN} (min^{-1})	τ (min)	R^2
400	2	10	0.113	34.805	0.975
400	2	15	0.118	24.872	0.956
400	2	20	0.112	21.241	0.978
400	2	25	0.132	16.840	0.975
400	1	15	0.115	13.982	0.984
400	2	15	0.118	24.872	0.956
400	3	15	0.146	35.164	0.98
400	4	15	0.152	37.171	0.996
200	2	15	0.143	38.986	0.989
400	2	15	0.118	24.872	0.956
600	2	15	0.146	20.041	0.946

Table 3
Parameters predicted by Adams–Bohart model

Influent concentration (mg/L)	Flow rate (mL/min)	Bed height (cm)	K_{ab} (L/mg min) (10^{-5})	N_0 (g/L)	R^2
400	10	2	15.8	20.647	0.863
400	15	2	9.0	20.944	0.902
400	20	2	8.0	19.750	0.794
400	25	2	7.0	19.100	0.683
400	15	1	4.75	20.336	0.819
400	15	2	9.0	20.944	0.902
400	15	3	20.3	20.340	0.851
400	15	4	22.8	20.571	0.902
200	15	2	45.0	10.471	0.914
400	15	2	9.0	20.944	0.902
600	15	2	5.17	29.670	0.853

of determination obtained for Adams–Bohart model are varying from 0.698 to 0.87 which depicts that this model moderately fits with the experimental data. Increase in the adsorption capacity of the nanocomposite with an increase in bed height, decrease in flow rate, and metal ion concentration was observed as it was found similar to the studies with rice husk ash [14]. The studies reveal that the experimental data strongly fits with Yoon–Nelson model with high value of coefficient of determination for varying influent concentrations, bed heights and flow rates similar
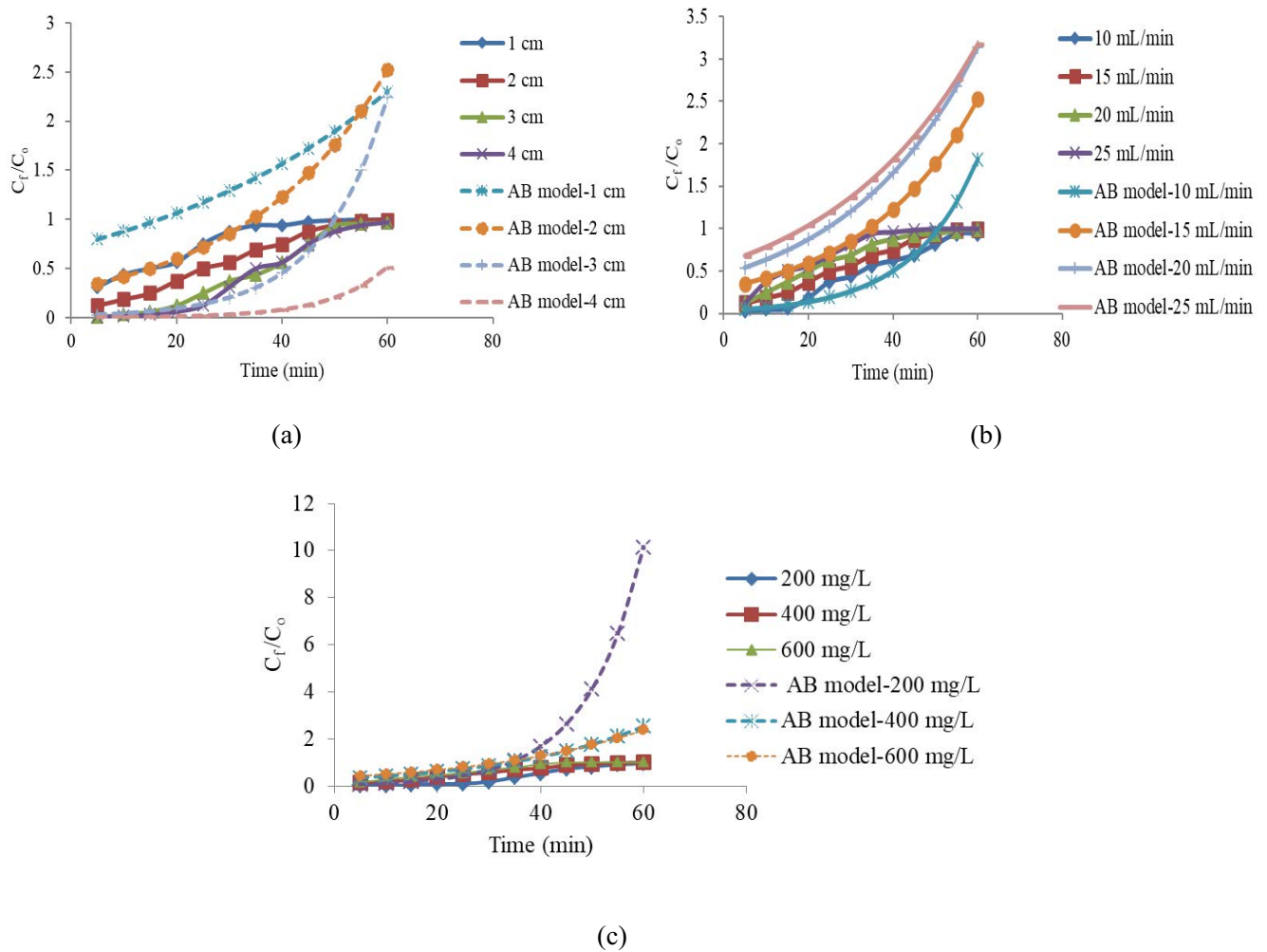
Fig. 13. (a–c) Experimental and theoretical breakthrough curves by Adams–Bohart model.

Table 4
Comparison of models

Influent concentration (mg/L)	Bed height (cm)	Flow rate (mL/min)	R^2 (Thomas model)	R^2 (Yoon–Nelson model)	R^2 (Adams–Bohart model)
400	2	10	0.681	0.975	0.791
400	2	15	0.736	0.982	0.870
400	2	20	0.886	0.994	0.708
400	2	25	0.891	0.979	0.698
400	1	15	0.877	0.974	0.770
400	2	15	0.736	0.982	0.870
400	3	15	0.477	0.983	0.7630
400	4	15	0.417	0.992	0.715
200	2	15	0.394	0.997	0.766
400	2	15	0.736	0.982	0.870
600	2	15	0.711	0.955	0.807

to the experimental studies of Cu(II) removal with lignocellulosic wastes [21].

4. Conclusion

The adsorption column experimental studies with varying bed heights of 1, 2, 3, and 4 cm of PPy/Al_2O_3-Fe_2O_3 nanocomposite indicates that as the bed height increases there is an increase in the breakthrough time. At a bed height of 4 cm maximum uptake was obtained due to higher surface area and thereby to treat more quantity of influent with metal ions. The effect of flow rate with 10, 15, 20 and 25 mL/min in the uptake of copper by PPy/Al_2O_3-Fe_2O_3 nanocomposite was studied and found early breakthrough time and saturation of bed media occurring at higher flow rate of 25 mL/min resulting in less adsorption intake. The best performance of the column is obtained at a lower flow rate and higher residence time. Adsorption studies conducted for the removal of Cu(II) with concentrations of 200, 400 and 600 mg/L indicate that a faster exhaustion of the adsorbent has taken place due to the saturation of active adsorptive sites at higher concentration. Breakthrough curves with higher bed height, low flow rate and initial concentration showed that more volume of feed could be treated through fixed bed adsorption column. Mathematical modelling showed that Yoon–Nelson model fits well with the experimental data obtained for copper removal through column adsorption studies. Hence it can be concluded that PPy/Al_2O_3-Fe_2O_3 nanocomposite is having high adsorption capacity to remove copper ions through packed bed column system within a short period of time.

References

[1] A.M. Tahir, A.A. Alazba, M.N. Amin, Absorption behaviours of copper, lead, and arsenic in aqueous solution using date palm fibres and orange peel: kinetics and thermodynamics, Pol. J. Environ. Stud., 26 (2017) 543–557.

[2] H.N.M. Ekramul Mahmud, S. Hosseini, R.B. Yahya, Polymer adsorbent for the removal of lead ions from aqueous solution, Int. J. Tech. Res. Appl., 11 (2014) 4–8.

[3] F. Gulshan, K. Okada, Preparation of alumina-iron oxide compounds by coprecipitation method and its characterization, Am. J. Mater. Sci. Eng., 201 (2013) 6–11.

[4] G.M. Al-Senani, F.F. Al-Fawzan, Study on adsorption of Cu and Ba from aqueous solutions using nanoparticles of *Origanum* (OR) and *Lavandula* (LV), Bioinorg. Chem. Appl., 11 (2018) 1–8, doi: 10.1155/2018/3936178.

[5] P. Heera, S. Shanmugam, Nanoparticle characterization and application: an overview, Int. J. Curr. Microbiol. Appl. Sci., 4 (2015) 379–386.

[6] Z. Melichová, L. Hromada, Adsorption of Pb^{2+} and Cu^{2+} ions from aqueous solutions on natural bentonite, Pol. J. Environ. Stud., 22 (2013) 457–464.

[7] C. Boukhalfa, A. Mennour, L. Reinert, M. Dray, L. Duclaux, Removal of copper from aqueous solutions by coprecipitation with hydrated iron oxide, Asian J. Chem., 19 (2007) 4267–4276.

[8] C.M. Hasfalina, R.Z. Maryam, C.A. Luqman, M. Rashid, Adsorption of copper(II) from aqueous medium in fixed-bed column by kenaf fibres, APCBEE Procedia, 3 (2012) 255–263.

[9] M.M. Abd El-Latif, A.M. Ibrahim, M.S. Showman, R.R. Abdel Hamide, Alumina/iron oxide nano composite for cadmium ions removal from aqueous solutions, Int. J. Nonferrous Metall., 2 (2013) 47–62.

[10] N. Ahmed, S.A. Reyad, Using polypyrrole nanocomposites coated on rice husk ash for the removal of anions, heavy metals, COD from textile wastewater, HBRC J., 13 (2017) 297–301.

[11] A. Mehdinia, S. Shegefti, F. Shemirani, Removal of lead(II), copper(II) and zinc(II) ions from aqueous solutions using magnetic amine-functionalized mesoporous silica nanocomposites, Chem. Eng. J., J. Braz. Chem. Soc., 26 (2015) 2249–2257.

[12] M. Nuria, C. Valderrama, I. Casas, M. Martínez, A. Florido, Cadmium and lead removal from aqueous solution by grape stalk wastes: modelling of a fixed-bed column, J. Chem. Eng. Data, 55 (2010) 3548–3554.

[13] F. Ostovar, R. Ansari, H.F. Moafi, Preparation and application of silver oxide/sawdust nanocomposite for chromium(VI) ion removal from aqueous solutions using column system, Global Nest J., 19 (2017) 1–11.

[14] S. Sarkar, S.K. Das, Removal of Cr(VI) and Cu(II) ions from aqueous solution by rice husk ash—column studies, Desal. Water Treat., 57 (2016) 20340–20349.

[15] S. Sugashini, K.M. Meera Sheriffa Begum, Column adsorption studies for the removal of Cr(VI) ions by ethylamine modified chitosan carbonized rice husk composite beads with modelling and optimization, J. Chem., 2013 (2013) 460971 (1–11), doi: 10.1155/2013/460971.

[16] I. Khan, K. Saeed, I. Khan, Nanoparticles: properties, applications and toxicities, Arabian J. Chem., 12 (2019) 908–931.

[17] M.A. Chougule, S.G. Pawar, P.R. Godse, R.N. Mulik, S. Sen, V.B. Patil, Synthesis and characterization of polypyrrole (PPy) thin films, Soft Nanosci. Lett., 1 (2011) 6–10.

[18] B.C. Pattanayak, Synthesis and Characterization of Alumina/Iron Oxide Mixed Nanocomposite, Master of Science-Thesis, National Institute of Technology, Rourkela, 2010.

[19] C. Sukumar, V. Janaki, K. Vijayaraghavan, S. Kamala-Kannan, K. Shanthi, Removal of Cr(VI) using co-immobilized activated carbon and *Bacillus subtilis*: fixed-bed column study, Clean Technol. Environ. Policy, 19 (2016) 251–258.

[20] E. El Hamidi, S. Arsalane, M. Halim, Kinetics and isotherm studies of copper removal by brushite calcium phosphate: linear and non-linear regression comparison, J. Chem., 9 (2012) 1532–1542, doi: 10.1155/2012/928073.

[21] Z.Z. Chowdhury, S.B. Abd Hamid, S.M. Zain, Evaluating design parameters for breakthrough curve analysis and kinetics of fixed bed columns for Cu(II) cations using lignocellulosic wastes, BioResources, 10 (2014) 732–749.